COLD SPRING HARBOR
Molecular Case Studies

RESEARCH ARTICLE

Identification of a novel large multigene deletion and a frameshift indel in *PDE6B* as the underlying cause of early-onset recessive rod–cone degeneration

Riccardo Sangermano,[1,4] Pooja Biswas,[2,4] Lori S. Sullivan,[3] Emily M. Place,[1] Shyamanga Borooah,[2] Juerg Straubhaar,[1] Eric A. Pierce,[1] Stephen P. Daiger,[3] Kinga M. Bujakowska,[1] and Radha Ayaggari[2]

[1]Ocular Genomics Institute, Massachusetts Eye and Ear Infirmary, Department of Ophthalmology, Harvard Medical School, Boston, Massachusetts 02114, USA; [2]Shiley Eye Institute, University of California San Diego, La Jolla, California 92093, USA; [3]Human Genetics Center, School of Public Health, University of Texas Health Science Center at Houston, Houston, Texas 77030, USA

Abstract A family, with two affected identical twins with early-onset recessive inherited retinal degeneration, was analyzed to determine the underlying genetic cause of pathology. Exome sequencing revealed a rare and previously reported causative variant (c.1923_1969delinsTCTGGG; p.Asn643Glyfs*29) in the *PDE6B* gene in the affected twins and their unaffected father. Further investigation, using genome sequencing, identified a novel ~7.5-kb deletion (Chr 4:670,405–677,862del) encompassing the *ATP5ME* gene, part of the 5′ UTR of *MYL5*, and a 378-bp (Chr 4:670,405–670,782) region from the 3′ UTR of *PDE6B* in the affected twins and their unaffected mother. Both variants segregated with disease in the family. Analysis of the relative expression of *PDE6B*, in peripheral blood cells, also revealed a significantly lower level of *PDE6B* transcript in affected siblings compared to a normal control. *PDE6B* is associated with recessive rod–cone degeneration and autosomal dominant congenital stationary night blindness. Ophthalmic evaluation of these patients showed night blindness, fundus abnormalities, and peripheral vision loss, which are consistent with *PDE6B*-associated recessive retinal degeneration. These findings suggest that the loss of *PDE6B* transcript resulting from the compound heterozygous pathogenic variants is the underlying cause of recessive rod–cone degeneration in the study family.

[Supplemental material is available for this article.]

INTRODUCTION

Autosomal recessive rod–cone degeneration (arRCD) is a genetically heterogeneous inherited retinal disease (IRD), affecting approximately 1 in 4000 individuals worldwide (Hartong et al. 2006). At least 46 loci associated with arRCD have been reported, and 44 of these genes have been identified so far (RetNet; https://sph.uth.edu/RetNet/). Pathogenic variants in some of these genes are also associated with multiple phenotypes including syndromic and nonsyndromic inherited RCD (Ferrari et al. 2011; Roosing et al. 2014). Furthermore, a few of these genes such as *CRX* and *PRPH2* are implicated in both dominant and recessive retinal

[4]These authors contributed equally to this work.

Corresponding author: rayyagari@health.ucsd.edu; kinga_bujakowska@meei.harvard.edu

Ontology terms: peripheral visual field loss; progressive visual field defects; severe visual impairment

Published by Cold Spring Harbor Laboratory Press

doi:10.1101/mcs.a006247

degenerations (Sankila et al. 2000; Sullivan et al. 2006; Coussa et al. 2015). Overall, a broad genetic and phenotypic variation has been observed in these diseases.

Pathogenic variants in known genes explain arRCD pathology in ~60% of recessive cases (Perez-Carro et al. 2016; Bujakowska et al. 2017; Weisschuh et al. 2020; Zampaglione et al. 2022). Based on current evidence, it is likely that the causative variants in the remaining 40% of cases involve sequence changes in the noncoding regions or alterations that are challenging to find by routine methodologies in genes previously implicated in IRD rather than novel genes (Bujakowska et al. 2017). Genome analysis has enabled the identification of coding and noncoding variants in both known and novel genes improving the outcome of mutation discovery studies.

Here, we describe the genetic analysis of a family that includes a set of twins affected by recessive retinal degeneration. We describe the detection of compound heterozygous variants in the *PDE6B* gene, including a known insertion–deletion (indel) and a novel large deletion involving three different genes, which segregate with disease.

RESULTS

Clinical Presentation and Family History

An RCD family (OGI773) with two affected sisters was recruited (Fig. 1). The mother reported European ancestry, whereas the father reported Jewish and European ancestry. Cases 1511 and 1513 were 29-yr-old female twins, who presented with progressive impairment of night vision and reduced peripheral vision, at 18 yr. However, they both reported to have had mild visual symptoms in the first decade of life. Their past medical histories were unremarkable. They were born as homozygotic twins from an uncomplicated delivery from a

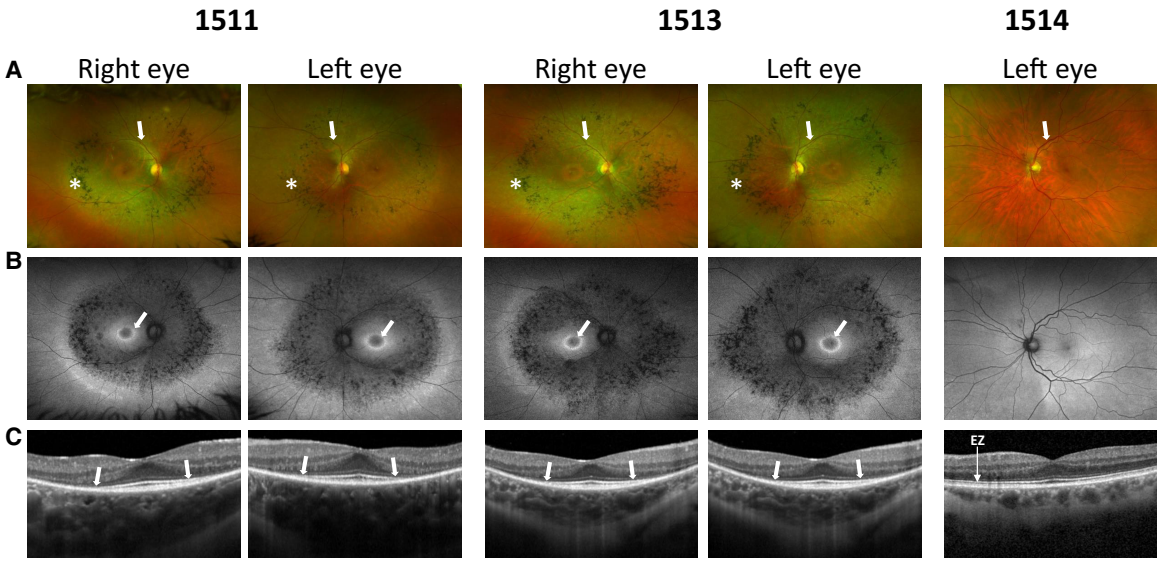

Figure 1. Imaging of left and right eyes of cases (1511 and 1513) and left eye of unaffected father (1514). (*A*) Widefield pseudocolor fundus imaging showed dark bone-spicule pigmentation (asterisk) and mild attenuation of retinal arterioles in both eyes (arrow), compared to the unaffected control. (*B*) Widefield fundus autofluorescence imaging showed reduced patchy autofluorescence in the areas of pigmentation. A ring of increased autofluorescence (arrow) was also observed in the parafovea bilaterally. (*C*) Spectral domain optical coherence tomography lines scans encompassing the fovea showed a loss of the ellipsoid zone (EZ) in the peripheral macula in the cases (arrows), compared to normal EZ in the unaffected control.

nonconsanguineous marriage. They had no systemic disease, were otherwise well, and had no history of use of medications associated with toxic retinopathy.

At her examination, individual 1511 had best corrected visual acuity of 20/20 in the right eye and 20/25 in the left eye. Her sister, 1513, had a best corrected visual acuity of 20/25 in the right eye and 20/35 in the left eye. Anterior segment examination was normal with an intraocular pressure within normal limits bilaterally for both. Fundus examination for both revealed a normal optic disc, with mild attenuation of retinal arterioles in both eyes. The most prominent finding was bilateral midperipheral bone-spicule type pigmentation encompassing the temporal retinal vascular arcades and encircling temporally and nasally in both eyes of both affected cases (Fig. 1A). Reduced patchy autofluorescence was noted on fundus autofluorescence imaging in the areas of pigmentation and also encroaching into the macula. A ring of increased autofluorescence was seen in the parafovea bilaterally (Fig. 1B). Spectral domain optical coherence tomography (SD-OCT) showed a posterior vitreous detachment and mild epiretinal membrane in both eyes of the affected twins. Additionally, there was loss of the ellipsoid zone—namely, the layer corresponding to the inner/outer segment of photoreceptors, peripherally at the clivus and loss of the external limiting membrane just peripheral to the clivus (Fig. 1C). The parents did not report visual symptoms; however, only the father, 1514, was clinically evaluated in a retinal clinic (Fig. 1).

Detection of a Novel Large *PDE6B* Deletion

Exome sequencing (ES) analysis of affected twins initially detected only one heterozygous pathogenic variant in *PDE6B*, c.1923_1969delinsTCTGGG, resulting in a frameshift and premature stop codon formation (p.Asn643Glyfs*29) within the phosphodiesterase catalytic domain (Table 1). This variant was absent in gnomAD and previously reported in several IRD patients (Supplemental Table S1; Shen et al. 2014; Ellingford et al. 2016; Carss et al. 2017; Haer-Wigman et al. 2017; Jespersgaard et al. 2019; Khateb et al. 2019; Jauregui et al. 2020; Weisschuh et al. 2020; Kuehlewein et al. 2021). We have classified it as pathogenic according to the American College of Medical Genetics and Genomics (ACMG) and the Association for Molecular Pathology (AMP) guidelines using the following criteria (loss-of-function variant, PVS1, detected in *trans* with a pathogenic variant, PM3, absent in population databases, PM2_SUPP) (Table 1). Segregation analysis confirmed the paternal transmission of this variant (Fig. 2).

No other high-impact likely pathogenic variants in currently known IRD genes (RetNet, https://sph.uth.edu/RetNet/) segregating with the phenotype were found (Supplemental Table S2).

Analysis of the ES and genome sequencing (GS) reads revealed a putative ~7.5-kb deletion in the 3′ UTR of *PDE6B* in the mother and the affected twins (Supplemental Fig. S1) that

Table 1. Variant information

Gene	Chromosome	HGVS DNA reference	HGVS protein reference	Variant type	Predicted effect	Genotype	Parent of origin	Comments
PDE6B	4	c.1923_1969delinsTCTGGG	p.(Asn643Glyfs*29)	Deletion/ insertion	Frameshift	Heterozygous	Father	Pathogenic (PVS1, PM2_SUPP, PM3)
PDE6B	4	Chr 4:670405-677862del	p.(?)	Deletion	3′-UTR truncation	Heterozygous	Mother	Pathogenic (PVS1,PS3)

Variants have been classified as pathogenic according to the American College of Medical Genetics and Genomics (ACMG) and the Association for Molecular Pathology (AMP) guidelines using the following criteria (loss-of-function variant, PVS1; deleterious effect confirmed by functional studies, PS3; detected in *trans* with a pathogenic variant, PM3; absent in population databases, PM2_SUPP).

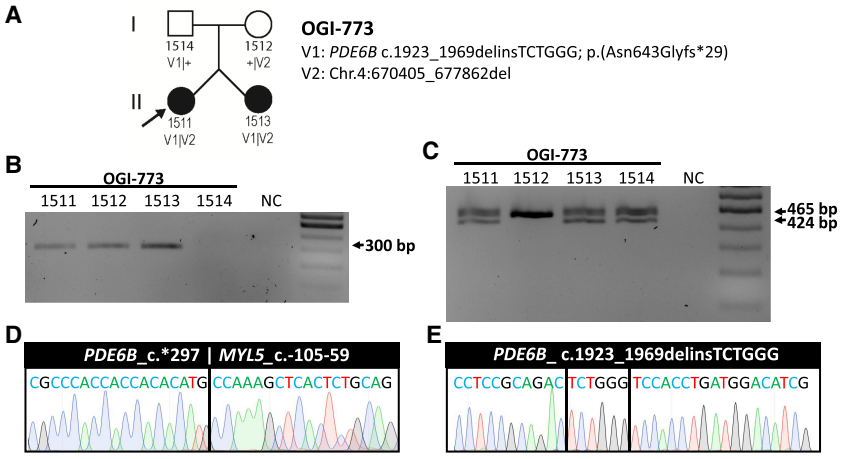

Figure 2. Pedigree of the rod–cone degeneration (RCD) family OGI-773 and segregation analysis of causal variants. (*A*) Affected twins are represented with black circles and proband is indicated by a black arrow. Patients are compound heterozygotes for one small *PDE6B* deletion/insertion causing frameshift (V1) and one larger ~7.5-kb deletion on Chromosome 4 (V2) encompassing the *PDE6B* 3′ UTR and downstream genomic segment. All presented variants refer to the *PDE6B* transcript NM_000283.4. (*B*,*D*) The large deletion Chr 4:670405–677862del, shown as a 300-bp polymerase chain reaction (PCR) fragment, was inherited from the unaffected mother. (*C*,*E*) The c.1923_1969delinsTCTGGG results in a smaller 424-bp band compared to the wild-type amplicon (465 bp). Unaffected father was carrier for this variant. (NC) Negative control.

was later confirmed by polymerase chain reaction (PCR) (Table 1; Fig. 2). This deletion (Chr 4: g.670,405–677,862del) removes part of the 3′ UTR of *PDE6B*, together with the ATP Synthase Membrane Subunit E (*ATP5ME*) and part of the 5′ UTR of *MYL5*. Because the mother does not present with an ocular phenotype, haploinsufficiency of the *ATP5ME* and the *MYL5* genes is not likely to be causal. The partial 378-bp deletion of the 3′ UTR of *PDE6B* in *trans* with the frameshift variant c.1923_1969delinsTCTGGG (p.Asn643Glyfs*29) were the most likely cause of the retinal phenotype in the affected cases.

Relative Expression of *PDE6B*

To investigate if a 378-bp deletion of the *PDE6B* 3′ UTR leads to decreased expression of *PDE6B*, we investigated mRNA expression in peripheral blood samples (Fig. 3). The peripheral blood mRNA of affected siblings, the unaffected father of the study family, and an unrelated normal control were isolated to analyze the expression profile of *PDE6B*. The level of *PDE6B* transcript was significantly decreased in the proband (1511) ($P < 0.0001$) and her affected twin sister (1513) ($P < 0.0001$) compared to the unrelated unaffected control. Further, the level of *PDE6B* transcript was also significantly lower in 1511 ($P = 0.001$) and 1513 ($P = 0.0007$), compared to their unaffected father (1514). Interestingly, the expression of *PDE6B* was also significantly lower in the unaffected father ($P = 0.0007$), carrying the c.1923_1969delinsTCTGGG (p.Asn643Glyfs*29) in the heterozygous state compared to the level of expression observed in the normal control (Fig. 3). We have classified this variant as pathogenic according to the ACMG/AMP guidelines using the following criteria (loss-of-function variant, PVS1, deleterious effect confirmed by functional studies, PS3) (Table 1).

DISCUSSION

We describe a family with twins affected with RCD, harboring compound heterozygous variants in the *PDE6B* gene. Although the p.Asn643Glyfs*29 is a known pathogenic variant, the

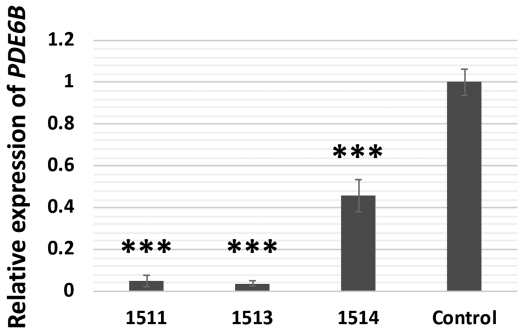

Figure 3. Relative expression levels of the *PDE6B* transcript in both affected sisters, unaffected father, and control sample. *PDE6B* expression was evaluated by quantitative polymerase chain reaction (qPCR) using peripheral blood mononuclear cell (PBMC)-extracted RNA. Significant decrease in the expression of *PDE6B* ($P < 0.0001$) was observed in both affected sisters 1511 and 1513 compared to the healthy control individual. The expression level of *PDE6B* transcript was also significantly lower in both affected sisters ($P = 0.001$ and $P = 0.0007$, respectively) compared to the level of transcript in their unaffected father 1514. The expression of *PDE6B* is also significantly lower in the unaffected father ($P = 0.0007$) carrying the c.1923_1969delinsTCTGGG (p.Asn643Glyfs*29) in the heterozygous state compared to the level of expression observed in normal control.

large 7.5-kb deletion (Chr 4:g.670,405–677,862del) is novel. Evidence of this variant was found through detailed manual review of the ES reads and was only clearly identified with GS. The RCD phenotype of these patients is consistent with the one associated with *PDE6B* in the literature, and it matches with the phenotype of patients harboring the known p.Asn643Glyfs*29 variant (Shen et al. 2014; Ellingford et al. 2016; Carss et al. 2017; Haer-Wigman et al. 2017; Jespersgaard et al. 2019; Khateb et al. 2019; Jauregui et al. 2020; Weisschuh et al. 2020; Kuehlewein et al. 2021).

Although the impact of the loss of a portion of the 3′ UTR of *PDE6B* is unknown, the Chr 4: g.670,405–677,862del does not disrupt the *PDE6B* coding sequence. However, this deletion could alter gene expression if the deleted region is involved in regulation. Quantitative PCR (qPCR) analysis using peripheral blood mononuclear cell (PBMC)-extracted RNA of both affected twins confirmed this hypothesis, as *PDE6B* expression was significantly decreased ($P < 0.0001$) compared to the control samples. Their unaffected father, carrying the heterozygous p.Asn643Glyfs*29 variant alone, also demonstrated a significant reduction of *PDE6B* expression ($P = 0.0007$) when compared with the expression in an unaffected control individual. However, the level of expression of *PDE6B* in unaffected father with a heterozygous wild-type allele is significantly higher compared to the expression levels in affected siblings with compound heterozygous mutations.

Although qPCR data suggest that *PDE6B* variants alone were sufficient to cause the RCD phenotype, the potential contribution of the heterozygous deletion of *ATP5ME* and *MYL5* to retinal disease is unknown. Currently, these two genes have never been associated to any disease phenotype. Our data suggest that haploinsufficiency of the *ATP5ME* and the *MYL5* is not likely to be causal, yet we do not have evidence to rule out a possible role of these genes in a recessive form of retinal degeneration. In addition, the large deletion may alter the topologically associated chromatin domains in the region that may affect surrounding gene expression (Rao et al. 2014). In fact, recent evidence has shown that large deletions in intergenic regions may alter gene expression by perturbing the finely regulated and self-interacting topological associating chromatin domains that share the same transcriptional units, by disrupting, removing or rearranging the protein binding sequences needed to demarcate those functional units (Lupiáñez et al. 2015; Franke et al. 2016; Spielmann et al. 2018; de Bruijn et al. 2020; Ibrahim and Mundlos 2020).

Incomplete molecular diagnosis is quite common in ophthalmic genetics, as at least 30%–40% of IRD patients remain genetically unexplained following conventional genetic testing (Abu-Safieh et al. 2013; Xu et al. 2014; Tiwari et al. 2016; Haer-Wigman et al. 2017; Villanueva-mendoza et al. 2021; Falsini et al. 2022). Thus, this study highlights the clinical and molecular importance of integrating GS and gene expression analyses into diagnostic pipelines. We successfully analyzed the *PDE6B* expression, using PBMCs as a source of RNA, even though the average expression of this gene in whole blood is only ~1 transcript per million (TPM), as indicated in the GTEx portal (https://gtexportal.org). Thus, our results encourage the use of a more accessible specimen, such as whole blood, to investigate altered expression or splicing defects of IRD genes (Shankar et al. 2015; Chen et al. 2018; Mihalich et al. 2022). GS alone also increases the diagnostic yield by detecting structural variations in known disease associated genes (Fadaie et al. 2021), and rare noncoding variants that may lead to altered gene expression or splicing defects.

In conclusion, we were able to provide complete molecular diagnosis of RCD in a set of twins and describe a novel, large deletion in *PDE6B*. This result carries an important significance as precise molecular diagnosis enables patients to be enrolled in gene therapy clinical trials or receive approved treatments (Russell et al. 2017; Fuller-Carter et al. 2020). A clinical trial for the *PDE6B*-associated disease is currently underway (NCT03328130), and thus depending on the outcome of this trial the molecular diagnosis can be clinically actionable for the described patients.

METHODS

Clinical Evaluation

A full dilated ophthalmological examination was performed that included assessment of best corrected visual acuity (BCVA) using a LogMAR vision chart at 4 m and measurements converted to Snellen visual acuity. Spectacle correction or a pinhole was used to achieve best corrected visual acuity. Additionally, slit lamp biomicroscopy and ophthalmoscopy was performed. Multimodal imaging was also performed, which included an SD-OCT (Heidelberg Engineering Inc.), widefield pseudocolor photos, and fundus autofluorescence (FAF) (Optos Inc.).

The study was approved by both the University of California San Diego and Massachusetts Eye and Ear, Mass General Brigham institutional review boards (IRBs) and adhered to the Declaration of Helsinki. Informed consent was obtained from all individuals on whom genetic testing and further molecular evaluations were performed.

Genetic Analysis

Blood samples were obtained from the proband (1511), her affected twin (1513), and their unaffected parents (1512, mother; 1514, father). Genomic DNA was isolated from peripheral blood lymphocytes by standard procedures.

ES was performed at the Center for Mendelian Genomics at the Broad Institute of the Massachusetts Institute of Technology and Harvard using methodology described previously (Zampaglione et al. 2022). ES data were aligned to hg38 and variants were called using the GATK HaplotypeCaller package version 3.5 (https://software.broadinstitute.org/gatk/). Data were displayed and analyzed with an online tool (https://seqr.broadinstitute.org).

The proband and her parents also underwent GS according to previously published protocols (Chaisson et al. 2019). In these patients, structural variants (SVs) were interrogated by GATK-SV package (Collins et al. 2020) and direct inspection of the read data using the

integrated genomic viewer (IGV) (Robinson et al. 2011). Coverage for both ES and GS samples can be found at Supplemental Table S3.

Guidelines of the American College of Medical Genetics (Richards et al. 2015) were used for the interpretation of sequence variants. Variants were verified to have an allele frequency of <1% in the Genome Aggregation Database (gnomAD; https://gnomad.broadinstitute.org/) (Karczewski et al. 2020).

Variant Validation

Variant segregation was performed by direct Sanger sequencing and analysis of next-generation sequencing (NGS) reads (Supplemental Fig. S1). Genomic DNA was amplified using Phusion High-Fidelity DNA Polymerase (New England Biolabs M0530) and primers flanking the deletions (Supplemental Table S4).

To sequence the *PDE6B* c.1923_1969delinsTCTGGG region, the full-length and smaller PCR amplicons were first cloned into the pCR2.1 plasmid by TA-cloning kit (Invitrogen 45-0046) (see Supplemental Table S4). Sanger sequencing was performed on ABI 3730xl (Applied Biosystems) using BigDye Terminator v3.1 kits (Life Technologies 4337455). Sequence analysis was done using SeqManPro (Lasergene 11, DNAStar).

mRNA Extraction and qRT-PCR

A minimum of 2.5 mL whole blood samples was collected in PAXgene Blood RNA tubes. Extraction of mRNA was performed using PAXgene Blood RNA Kit (PreAnalytiX GmbH 762174) by following the company instruction.

The cDNA synthesis and qPCR analysis of the *PDE6B* gene to the housekeeping genes *GAPDH* and *ACTB* were performed as described earlier (Mandal et al. 2006) (qPCR primers and C_t values are listed in Supplemental Tables S4 and S5, respectively). For the experimental data sets, the mean and standard deviation were calculated, and the significance was calculated using the Student's *t*-test. The *P*-value < 0.0001 was indicated by *** and determined as statistically significant.

ADDITIONAL INFORMATION

Data Deposition and Access

The novel causal variant identified in the present study has been deposited to ClinVar (https://www.ncbi.nlm.nih.gov/clinvar/) and can be found under accession number SCV002589126. Exome and genome sequencing data have been deposited in the NCBI database of Genotypes and Phenotypes (dbGaP) (Submission IDs phs002459.v1.p1 and phs002459.v1.p1, respectively).

Ethics Statement

The study was approved by the institutional review board at the Massachusetts Eye and Ear (MEE), an affiliate of Mass General Brigham (MGB) healthcare system (Human Studies Committee MGB, Boston), the IRB of the UC San Diego and complied with the Health Information Portability and Accessibility Act (HIPAA). All aspects of the project adhered to the tenets of the Declaration of Helsinki. Informed consent was obtained from all individuals on whom genetic analysis and further molecular evaluations were performed.

Acknowledgments

The authors thank the patients and their family members for their participation in this study and the Ocular Genomics Institute Genomics Core members for their experimental

assistance. The authors thank the Exome Aggregation Consortium, the Genome Aggregation Database (gnomAD), and the groups that provided exome variant data for comparison. A full list of contributing groups can be found at http://exac.broadinstitute.org/about and http://gnomad.broadinstitute.org/about.

Author Contributions

R.S. and P.B. performed experiments and contributed to the writing of the manuscript. L.S.S. and J.S. provided data analysis. S.P.D. and E.A.P. reviewed the manuscript. S.B. and E.A.P. provided clinical data and reviewed the manuscript. K.M.B. and R.A. guided the experimental design, provided variant analysis, and contributed to the writing of the manuscript.

Funding

This work was supported by grants from the Foundation Fighting Blindness (EGI-GE1218-0753-UCSD to K.M.B., R.A., and S.D.; CD-GT-0918-0746-SE to S.B.), the National Eye Institute (RO1EY030591 [to R.A.], RO1EY031663 [to R.A.], RO1EY021237 [to R.A.], R01EY026904 [to K.M.B. and E.A.P.], R01EY012910 [to E.A.P.], P30EY014104 [MEEI core support], and P30EY022589 [core support, to R.A.]), Nixon Visions Foundation to R.A. and S.B., and Research to Prevent Blindness International Research Collaborators Award to K.M.B. Sequencing and analysis were provided by the Broad Institute of MIT and Harvard Center for Mendelian Genomics (Broad CMG) and was funded by the National Human Genome Research Institute, the National Eye Institute, and the National Heart, Lung and Blood Institute grant UM1HG008900 and in part by National Human Genome Research Institute grant R01HG009141.

Competing Interest Statement

The authors have declared no competing interest.

Received September 20, 2022; accepted in revised form November 2, 2022.

REFERENCES

Abu-Safieh L, Alrashed M, Anazi S, Alkuraya H, Khan AO, Al-Owain M, Al-Zahrani J, Al-Abdi L, Hashem M, Al-Tarimi S, et al. 2013. Autozygome-guided exome sequencing in retinal dystrophy patients reveals pathogenetic mutations and novel candidate disease genes. *Genome Res* **23:** 236–247. doi:10.1101/gr.144105.112

Bujakowska KM, Fernandez-Godino R, Place E, Consugar M, Navarro-Gomez D, White J, Bedoukian EC, Zhu X, Xie HM, Gai X, et al. 2017. Copy-number variation is an important contributor to the genetic causality of inherited retinal degenerations. *Genet Med* **19:** 643–651. doi:10.1038/gim.2016.158

Carss KJ, Arno G, Erwood M, Stephens J, Sanchis-Juan A, Hull S, Megy K, Grozeva D, Dewhurst E, Malka S, et al. 2017. Comprehensive rare variant analysis via whole-genome sequencing to determine the molecular pathology of inherited retinal disease. *Am J Hum Genet* **100:** 75–90. doi:10.1016/j.ajhg.2016.12.003

Chaisson MJP, Sanders AD, Zhao X, Malhotra A, Porubsky D, Rausch T, Gardner EJ, Rodriguez OL, Guo L, Collins RL, et al. 2019. Multi-platform discovery of haplotype-resolved structural variation in human genomes. *Nat Commun* **10:** 1784. doi:10.1038/s41467-018-08148-z

Chen X, Sheng X, Liu Y, Li Z, Sun X, Jiang C, Qi R, Yuan S, Wang X, Zhou G, et al. 2018. Distinct mutations with different inheritance mode caused similar retinal dystrophies in one family: a demonstration of the importance of genetic annotations in complicated pedigrees. *J Transl Med* **16:** 145. doi:10.1186/s12967-018-1522-7

Collins RL, Brand H, Karczewski KJ, Zhao X, Alföldi J, Francioli LC, Khera AV, Lowther C, Gauthier LD, Wang H, et al. 2020. A structural variation reference for medical and population genetics. *Nature* **581:** 444–451. doi:10.1038/s41586-020-2287-8

Coussa RG, Chakarova C, Ajlan R, Taha M, Kavalec C, Gomolin J, Khan A, Lopez I, Ren H, Waseem N, et al. 2015. Genotype and phenotype studies in autosomal dominant retinitis pigmentosa (adRP) of the French Canadian founder population. *Investig Ophthalmol Vis Sci* **56:** 8297–8305. doi:10.1167/iovs.15-17104

de Bruijn SE, Fiorentino A, Ottaviani D, Fanucchi S, Melo US, Corral-Serrano JC, Mulders T, Georgiou M, Rivolta C, Pontikos N, et al. 2020. Structural variants create new topological-associated domains and ectopic retinal enhancer-gene contact in dominant retinitis pigmentosa. *Am J Hum Genet* **107:** 802–814. doi:10.1016/j.ajhg.2020.09.002

Ellingford JM, Barton S, Bhaskar S, Williams SG, Sergouniotis PI, O'Sullivan J, Lamb JA, Perveen R, Hall G, Newman WG, et al. 2016. Whole genome sequencing increases molecular diagnostic yield compared with current diagnostic testing for inherited retinal disease. *Ophthalmology* **123:** 1143–1150. doi:10.1016/j.ophtha.2016.01.009

Fadaie Z, Whelan L, Ben-Yosef T, Dockery A, Corradi Z, Gilissen C, Haer-Wigman L, Corominas J, Astuti GDN, de Rooij L, et al. 2021. Whole genome sequencing and *in vitro* splice assays reveal genetic causes for inherited retinal diseases. *NPJ Genomic Med* **6:** 97. doi:10.1038/s41525-021-00261-1

Falsini B, Placidi G, De Siena E, Chiurazzi P, Minnella AM, Savastano MC, Ziccardi L, Parisi V, Iarossi G, Percio M, et al. 2022. Genetic characteristics of 234 Italian patients with macular and cone/cone-rod dystrophy. *Sci Rep* **12:** 3774. doi:10.1038/s41598-022-07618-1

Ferrari S, Di Iorio E, Barbaro V, Ponzin D, Sorrentino F S, Parmeggiani F. 2011. Retinitis pigmentosa: genes and disease mechanisms. *Curr Genomics* **12:** 238–249. doi:10.2174/138920211795860107

Franke M, Ibrahim DM, Andrey G, Schwarzer W, Heinrich V, Schöpflin R, Kraft K, Kempfer R, Jerković I, Chan WL, et al. 2016. Formation of new chromatin domains determines pathogenicity of genomic duplications. *Nature* **538:** 265–269. doi:10.1038/nature19800

Fuller-Carter PI, Basiri H, Harvey AR, Carvalho LS. 2020. Focused update on AAV-based gene therapy clinical trials for inherited retinal degeneration. *BioDrugs* **34:** 763–781. doi:10.1007/s40259-020-00453-8

Haer-Wigman L, Van Zelst-Stams WAG, Pfundt R, Van Den Born LI, Klaver CCW, Verheij JBGM, Hoyng CB, Breuning MH, Boon CJF, Kievit AJ, et al. 2017. Diagnostic exome sequencing in 266 Dutch patients with visual impairment. *Eur J Hum Genet* **25:** 591–599. doi:10.1038/ejhg.2017.9

Hartong DT, Berson EL, Dryja TP. 2006. Retinitis pigmentosa. *Lancet* **368:** 1795–1809. doi:10.1016/S0140-6736(06)69740-7

Ibrahim DM, Mundlos S. 2020. Three-dimensional chromatin in disease: what holds us together and what drives us apart? *Curr Opin Cell Biol* **64:** 1–9. doi:10.1016/j.ceb.2020.01.003

Jauregui R, Chan L, Oh JK, Cho A, Sparrow JR, Tsang SH. 2020. Disease asymmetry and hyperautofluorescent ring shape in retinitis pigmentosa patients. *Sci Rep* **10:** 3364. doi:10.1038/s41598-020-60137-9

Jespersgaard C, Fang M, Bertelsen M, Dang X, Jensen H, Chen Y, Bech N, Dai L, Rosenberg T, Zhang J, et al. 2019. Molecular genetic analysis using targeted NGS analysis of 677 individuals with retinal dystrophy. *Sci Rep* **9:** 1219. doi:10.1038/s41598-018-38007-2

Karczewski KJ, Francioli LC, Tiao G, Cummings BB, Alföldi J, Wang Q, Collins RL, Laricchia KM, Ganna A, Birnbaum DP, et al. 2020. The mutational constraint spectrum quantified from variation in 141,456 humans. *Nature* **581:** 434–443. doi:10.1038/s41586-020-2308-7

Khateb S, Nassisi M, Bujakowska KM, Méjécase C, Condroyer C, Antonio A, Foussard M, Démontant V, Mohand-Saïd S, Sahel JA, et al. 2019. Longitudinal clinical follow-up and genetic spectrum of patients with rod–cone dystrophy associated with mutations in *PDE6A* and *PDE6B*. *JAMA Ophthalmol* **137:** 669–679. doi:10.1001/jamaophthalmol.2018.6367

Kuehlewein L, Zobor D, Stingl K, Kempf M, Nasser F, Bernd A, Biskup S, Cremers FPM, Khan MI, Mazzola P, et al. 2021. Clinical phenotype of *PDE6B*-associated retinitis pigmentosa. *Int J Mol Sci* **22:** 2374. doi:10.3390/ijms22052374

Lupiáñez DG, Kraft K, Heinrich V, Krawitz P, Brancati F, Klopocki E, Horn D, Kayserili H, Opitz JM, Laxova R, et al. 2015. Disruptions of topological chromatin domains cause pathogenic rewiring of gene–enhancer interactions. *Cell* **161:** 1012–1025. doi:10.1016/j.cell.2015.04.004

Mandal MNA, Vasireddy V, Jablonski MM, Wang XF, Heckenlively JR, Hughes BA, Reddy GB, Ayyagari R. 2006. Spatial and temporal expression of MFRP and its interaction with CTRP5. *Investig Ophthalmol Vis Sci* **47:** 5514–5521. doi:10.1167/iovs.06-0449

Mihalich A, Cammarata G, Tremolada G, Pollazzon M, Di Blasio AM, Marzoli SB. 2022. Two novel *CACNA1F* gene mutations cause two different phenotypes: Aland eye disease and incomplete congenital stationary night blindness. *Exp Eye Res* **221:** 1–7. doi:10.1016/j.exer.2022.109143

Perez-Carro R, Corton M, Sánchez-Navarro I, Zurita O, Sanchez-Bolivar N, Sánchez-Alcudia R, Lelieveld SH, Aller E, López-Martínez MA, López-Molina MI, et al. 2016. Panel-based NGS reveals novel pathogenic mutations in autosomal recessive retinitis pigmentosa. *Sci Rep* **6:** 19531. doi:10.1038/srep19531

Rao SSP, Huntley MH, Durand NC, Stamenova EK, Bochkov ID, Robinson JT, Sanborn AL, Machol I, Omer AD, Lander ES, et al. 2014. A 3D map of the human genome at kilobase resolution reveals principles of chromatin looping. *Cell* **159:** 1665–1680. doi:10.1016/j.cell.2014.11.021

Richards S, Aziz N, Bale S, Bick D, Das S, Gastier-Foster J, Grody WW, Hegde M, Lyon E, Spector E, et al. 2015. Standards and guidelines for the interpretation of sequence variants: a joint consensus recommendation of the American College of Medical Genetics and Genomics and the Association for Molecular Pathology. *Genet Med* **17:** 405–424. doi:10.1038/gim.2015.30

Robinson JT, Thorvaldsdóttir H, Winckler W, Guttman M, Lander ES, Getz G, Mesirov JP. 2011. Integrative genomics viewer. *Nat Biotechnol* **29:** 24–26. doi:10.1038/nbt.1754

Roosing S, Thiadens AAHJ, Hoyng CB, Klaver CCW, den Hollander AI, Cremers FPM. 2014. Causes and consequences of inherited cone disorders. *Prog Retin Eye Res* **42:** 1–26. doi:10.1016/j.preteyeres.2014.05.001

Russell S, Bennett J, Wellman JA, Chung DC, Yu ZF, Tillman A, Wittes J, Pappas J, Elci O, McCague S, et al. 2017. Efficacy and safety of voretigene neparvovec (AAV2-hRPE65v2) in patients with *RPE65*-mediated inherited retinal dystrophy: a randomised, controlled, open-label, phase 3 trial. *Lancet* **390:** 849–860. doi:10.1016/S0140-6736(17)31868-8

Sankila EM, Joensuu TH, Hämäläinen RH, Raitanen N, Valle O, Ignatius J, Cormand B. 2000. A CRX mutation in a Finnish family with dominant cone-rod retinal dystrophy. *Hum Mutat* **16:** 94. doi:10.1002/1098-1004(200007)16:1<94::AID-HUMU25>3.0.CO;2-T

Shankar SP, Birch DG, Ruiz RS, Hughbanks-Wheaton DK, Sullivan LS, Bowne SJ, Stone EM, Daiger SP. 2015. Founder effect of a c.828+3A>T splice site mutation in peripherin 2 (*PRPH2*) causing autosomal dominant retinal dystrophies. *JAMA Ophthalmol* **133:** 511–517. doi:10.1001/jamaophthalmol.2014.6115

Shen S, Sujirakul T, Tsang SH. 2014. Next-generation sequencing revealed a novel mutation in the gene encoding the β subunit of rod phosphodiesterase. *Ophthalmic Genet* **35:** 142–150. doi:10.3109/13816810.2014.915328

Spielmann M, Lupiáñez DG, Mundlos S. 2018. Structural variation in the 3D genome. *Nat Rev Genet* **19:** 453–467. doi:10.1038/s41576-018-0007-0

Sullivan LS, Bowne SJ, Birch DG, Hughbanks-Wheaton D, Heckenlively JR, Lewis RA, Garcia CA, Ruiz RS, Blanton SH, Northrup H, et al. 2006. Prevalence of disease-causing mutations in families with autosomal dominant retinitis pigmentosa: a screen of known genes in 200 families. *Investig Ophthalmol Vis Sci* **47:** 3052–3064. doi:10.1167/iovs.05-1443

Tiwari A, Bahr A, Bähr L, Fleischhauer J, Zinkernagel MS, Winkler N, Barthelmes D, Berger L, Gerth-Kahlert C, Neidhardt J, et al. 2016. Next generation sequencing based identification of disease-associated mutations in Swiss patients with retinal dystrophies. *Sci Rep* **6:** 28755. doi:10.1038/srep28755

Villanueva-mendoza C, Tuson M, Apam-garduño D, De Castro-mir M, Tonda R, Trotta JR, Marfany G, Valero R, Cort V, Gonz R. 2021. The genetic landscape of inherited retinal diseases in a Mexican cohort: genes, mutations and phenotypes. *Genes (Basel)* **12:** 1824. doi:10.3390/genes12111824

Weisschuh N, Obermaier CD, Battke F, Bernd A, Kuehlewein L, Nasser F, Zobor D, Zrenner E, Weber E, Wissinger B, et al. 2020. Genetic architecture of inherited retinal degeneration in Germany: a large cohort study from a single diagnostic center over a 9-year period. *Hum Mutat* **41:** 1514–1527. doi:10.1002/humu.24064

Xu Y, Guan L, Shen T, Zhang J, Xiao X, Jiang H, Li S, Yang J, Jia X, Yin Y, et al. 2014. Mutations of 60 known causative genes in 157 families with retinitis pigmentosa based on exome sequencing. *Hum Genet* **133:** 1255–1271. doi:10.1007/s00439-014-1460-2

Zampaglione E, Maher M, Place EM, Wagner NE, DiTroia S, Chao KR, England E CMGB, Catomeris A, Nassiri S, et al. 2022. The importance of automation in genetic diagnosis: lessons from analyzing an inherited retinal degeneration cohort with the Mendelian Analysis Toolkit (MATK). *Genet Med* **24:** 332–343. doi:10.1016/j.gim.2021.09.015